Plant Physiol. (1989) 91, 749–755
0032-0889/89/91/749/07/$01.00/0

Received for publication April 19, 1989
and in revised form June 5, 1989

Short-Term Metabolite Changes during Transient Ammonium Assimilation by the *N*-Limited Green Alga *Selenastrum minutum*[1]

Ronald G. Smith, Greg C. Vanlerberghe, Mark Stitt, and David H. Turpin*

Department of Biology, Queen's University, Kingston, Ontario, Canada K7L 3N6 (R.G.S., G.C.V., D.H.T.), *and Lehrstuhl fur Pflanzenphysiologie, Universitat Bayreuth, D8580 Bayreuth, Federal Republic of Germany* (M.S.)

ABSTRACT

In this study, we measured the total pool sizes of key cellular metabolites from nitrogen-limited cells of *Selenastrum minutum* before and during ammonium assimilation in the light. This was carried out to identify the sites at which N assimilation is acting to regulate carbon metabolism. Over 120 seconds following NH_4^+ addition we found that: (a) N accumulated in glutamine while glutamate and α-ketoglutarate levels fell; (b) ATP levels declined within 5 seconds and recovered within 30 seconds of NH_4^+ addition; (c) ratios of pyruvate/phospho*enol*pyruvate, malate/phospho*enol*pyruvate, Glc-1-P/Glc-6-P and Fru-1,6-bisphosphate/Fru-6-P increased; and (d) as previously seen, photosynthetic carbon fixation was inhibited. Further, we monitored starch degradation during N assimilation over a longer time course and found that starch breakdown occurred at a rate of about 110 micromoles glucose per milligram chlorophyll per hour. The results are consistent with N assimilation occurring through glutamine synthetase/glutamate synthase at the expense of carbon previously stored as starch. They also indicate that regulation of several enzymes is involved in the shift in metabolism from photosynthetic carbon assimilation to carbohydrate oxidation during N assimilation. It seems likely that pyruvate kinase, phospho*enol*pyruvate carboxylase, and starch degradation are all activated, whereas key Calvin cycle enzyme(s) are inactivated within seconds of NH_4^+ addition to N-limited *S. minutum* cells. The rapid changes in glutamate and triose phosphate, recently shown to be regulators of cytosolic pyruvate kinase, are consistent with them contributing to the short-term activation of this enzyme.

Nitrogen is an important regulator of carbon flow in higher plants and algae (1, 18, 25). When the green alga *Selenastrum minutum* is cultured under N limitation, its capacity for NH_4^+ assimilation increases about ninefold (4, 5). It is therefore not surprising that the significance of N in regulating carbon flow increases upon N limitation (5, 25). In algae, N assimilation into amino acids occurs via the GS/GOGAT[2] pathway. This pathway requires αKG, ATP, and reducing power for its operation (3). Initiation of such high rates of NH_4^+ assimilation therefore requires large changes in cellular metabolism to meet the newly created demand for carbon skeletons, ATP, and reductant.

In the present study we have measured the total pool sizes of many of the potentially important cellular metabolites before and during NH_4^+ assimilation by the *N*-limited green alga *S. minutum*. This approach, as opposed to ^{32}P and ^{14}C radiolabel and ^{14}C pulse-chase techniques (5, 10), has allowed us to observe unambiguously the response of the overall level of the metabolite pools and therefore gain insights into the regulatory processes involved in carbon partitioning to NH_4^+ assimilation. Our results suggest that starch degradation, PEPcase, and PK are all activated within seconds after adding NH_4^+. Changes in Glu and triose-P, key regulators of PK in this alga (14), are consistent with them contributing to a rapid activation of PK. Short-term changes in FBP suggest that the decrease in Calvin cycle activity during NH_4^+ assimilation may be the result of direct inactivation of one or more of the Calvin cycle enzymes.

MATERIALS AND METHODS

Plant Material

Selenastrum minutum (Naeg.) Collins (UTEX 2459) was isolated from Lake Ontario, Kingston, Canada in 1984. It was cultured in NO_3^--limited chemostats in Kingston, Canada, as previously described (4).

Experimental

The cells were harvested from chemostats and concentrated to approximately 40 μg Chl·ml^{-1} by centrifugation (10,000*g*, 10 min). Cells were resuspended in the supernatant medium buffered with 25 mM Hepes (pH 8.0). Before sampling, the

[1] Supported by the Natural Sciences and Engineering Research Council of Canada (NSERC) and the Deutsche Forschungsgemeinschaft (SFB 137). G. C. V. acknowledges an NSERC postgraduate scholarship.

[2] Abbreviations: GS, glutamine synthetase (EC 6.3.1.2); GOGAT, glutamate synthase (EC 1.4.7.1); αKG, α-ketoglutarate; PEPcase, phospho*enol*pyruvate carboxylase (EC 4.1.1.31); PK, pyruvate kinase (EC 2.7.1.40); FBP, fructose-1,6-bisphosphate; PEP, phospho*enol*pyruvate; pyr, pyruvate; RuBP, ribulose-1,5-bisphosphate; PGA, phosphoglycerate; ETC, electron transport chain; TCAC, tricarboxylic acid cycle; FBPase, fructose-1,6-bisphosphatase (EC 3.1.3.11); PFK, phosphofructokinase (EC 2.7.1.11).

algal suspension was darkened and bubbled with air for 20 min. It was then transferred to a sampling vessel and preconditioned in light for 5 min in the presence of 58 mM $NaHCO_3$. The sampling vessel was a 50 mL Eppendorf repeater pipet containing a magnetic stir bar and fitted with an injection port. Illumination was provided by two projectors (Kodak Carousel 600H) and the light passed through a water bath which acted as a heat sink.

Samples were taken at successive times over a 3 min period, three samples preceding and five samples following the addition of NH_4Cl. NH_4Cl was added to a concentration of 3.4 mM, a concentration that has been shown not to uncouple photophosphorylation in *S. minutum* (4, 27). Samples (4 mL) were pipetted under continued illumination into liquid N_2-cooled 250 ml round bottom flasks, lyophilized and transported on dry ice to Bayreuth, FRG, for metabolite analyses.

Metabolite Assays

The freeze-dried material was extracted in 10% $HClO_4$ and neutralized with 5 N KOH/1 M triethanolamine. RuBP was assayed using the ^{14}C radiolabel incorporation technique (30). Amino acids were analyzed by HPLC (Kontron HPLC-System 400) using the fluorescent *o*-phthaldehyde postcolumn derivatization technique (21). The remaining metabolites were measured using standard coupled enzymatic assays (20, 30) and a dual-wavelength spectrophotometer (ZFP22, Sigma Instruments, FRG). αKG was assayed as in Bergmeyer (2) using 100 mM phosphate buffer (pH 7.5), 2 mM NH_4Cl, 5 mM NADH, starting the reaction by adding 1.2 units glutamate dehydrogenase. Isocitrate, citrate, and malate were measured as in Bergmeyer (2). Recovery experiments were carried out in which a representative amount of the metabolite was added to the frozen cells and extracted and assayed. The recovery of the added metabolites (as a percentage of that added) was Fru-6-P, 56%; Glc-1-P, 55%; ATP, 50%; AMP, 75%; triose-P, 57%, FBP, 64%; PGA, 61%; pyr, 51%; PEP, 80%.

To ensure that the Glc-1-P/Glc-6-P ratios determined were accurate, we measured Glc-1-P with two assays. First, Glc-1-P and Glc-6-P were measured by coupling these substrates to Glc-6-P oxidation as in Wirtz *et al.* (30). The assay mixture contained 0.25 mM NADP in 100 mM Tris buffer containing 5 mM $MgCl_2$ (pH 8.1). The reaction was initiated by adding 0.3 unit of Glc-6-P-dehydrogenase (EC 1.1.1.49) and 0.8 unit of phosphoglucomutase (EC 5.4.2.2). Glc-1-P was also measured by coupling it to UDPGlc oxidation in an assay adapted from that for UTP (20). The assay mixture contained 1 mM UTP and 0.15 mM NAD^+ in 200 mM glycine buffer containing 2 mM EDTA and 5 mM $MgCl_2$ (pH 8.7). The reaction was initiated by adding 0.01 unit of UDPGlc-dehydrogenase (EC 1.1.1.22) to remove UDPGlc, and then 3 units of UDPGlc-pyrophosphorylase.

An experiment of longer duration was conducted to determine the rates of starch and sucrose degradation during NH_4^+ assimilation. This was necessitated because the large pool sizes of these metabolites made it impossible to detect changes in their levels over short time periods. In these experiments the cells were used directly from a chemostat, about 1 μg Chl ml^{-1}. The cells were kept in a water-jacketed cuvette (20°C), illuminated by a projector (Kodak Carousel 600H), and bubbled with air. Samples (1 mL) were frozen in liquid N_2, lyophilized and extracted in $HClO_4$ as above. The samples were centrifuged (Eppendorf, 14,000*g*). The supernatant was neutralized and analyzed for Glc, Fru, and sucrose (2). As sucrose is partially hydrolyzed in acid, total sucrose was estimated as hexose equivalents by summing Glc, Fru, and twice the sucrose values. The pellet was resuspended in 400 μL of 0.02 N NaOH, sonicated for 20 s, and autoclaved for 20 min at 121°C and 14 psi. This treatment solubilized the starch and oxidized any contaminating Glc. The samples were then treated with α-amylase (10 units) and amyloglucosidase (1 unit) for 14 h at 55°C in 200 mM Na-acetate buffer (pH 5.0) (9). The Glc produced was analyzed as described previously (2).

Chl concentrations were estimated by measuring the phaeophytin content of the $HClO_4$ pellet (29).

RESULTS

The data reported are the mean values from three separate experiments. The variation about each data point is generally in the range of 10 to 15%. Most of this variation was due to interexperimental differences. The trends exhibited by the grouped data were also apparent in each replicate experiment. Metabolite recoveries were generally constant between all replicates and ranged from 50 to 80% (see "Materials and Methods").

Amino Acids and αKG

The addition of NH_4^+ to *N*-limited *S. minutum* results in rapid changes in many cellular metabolites. Glutamine levels rose steadily following NH_4^+-addition (Fig. 1). The net rate of glutamine production was 32 μmol N mg Chl^{-1} h^{-1} over the first 30 s and about 17 μmol N mg Chl^{-1} h^{-1} for the period 30 to 60 s following NH_4^+-addition. At the same time, glutamate and αKG levels fell rapidly for 15 s and then reached relatively stable levels. Of all the other detectable amino acids, only alanine increased slightly over the 2 min period (see Table I).

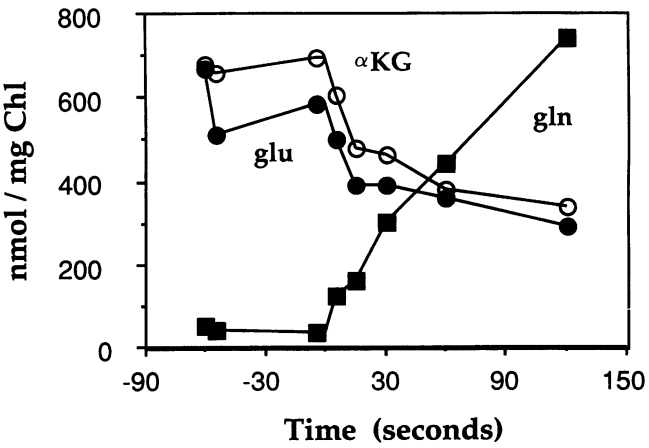

Figure 1. Changes in the cellular pool sizes of glutamine, glutamate, and αKG in response to NH_4^+ addition at time 0. The data points represent the means of three separate experiments.

Adenylates

ATP levels declined dramatically within 5 s following NH_4^+ addition and then recovered within 30 s nearly to the levels before N was added (Fig. 2). ADP and AMP showed reciprocal changes.

pyr, PEP, and Malate

Within 5 s of NH_4^+ addition, PEP levels fell by 50% and pyr levels increased twofold (Fig. 3A). Malate levels remained constant or declined slightly over this period. The ratios of pyr/PEP and malate/PEP increased by about seven- and threefold, respectively, following NH_4^+-addition (Fig. 3B).

FBP, Fru-6-P, Glc-1-P, and Glc-6-P

Immediately following NH_4^+ addition, FBP levels rose fivefold, whereas Fru-6-P levels remained relatively constant, resulting in a fivefold increase in the FBP/Fru-6-P ratio (Fig. 4, A and B). Similarly, Glc-1-P levels rose about threefold, whereas Glc-6-P levels remained relatively constant. Thus, upon NH_4^+ addition the Fru-6-P/Glc-6-P ratio did not change (not shown), while the Glc-1-P/Glc-6-P ratio rose threefold (Fig. 4, A and B). Use of the UDPGlc-DH assay confirmed the increase in the Glc-1-P/Glc-6-P ratio (data not shown).

Starch and Sucrose

N-Limited *S. minutum* cells have basal levels of starch and sucrose of about 500 and 8 μmol Glc mg Chl^{-1}, respectively. Upon NH_4^+ addition in illuminated cells both starch and sucrose levels fell. The net rate of Glc equivalents produced from starch degradation (110 μmol Glc mg Chl^{-1} h^{-1}; Fig. 5) during N-assimilation was greater than that from sucrose (3.5 μmol Glc mg Chl^{-1} h^{-1}; not shown). It must be noted that, for technical reasons, starch and sucrose were monitored over a longer time course than the other metabolites. This was unavoidable, due to the large pool sizes of these storage metabolites, and meant that there is no detectable decrease of the pool size over 120 s.

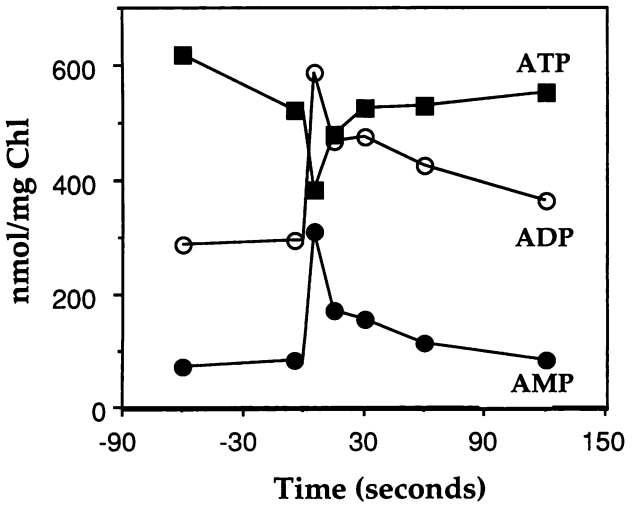

Figure 2. Changes in the cellular pool sizes of ATP, ADP, and AMP in response to NH_4^+ addition at time 0. The data points represent the means of three separate experiments.

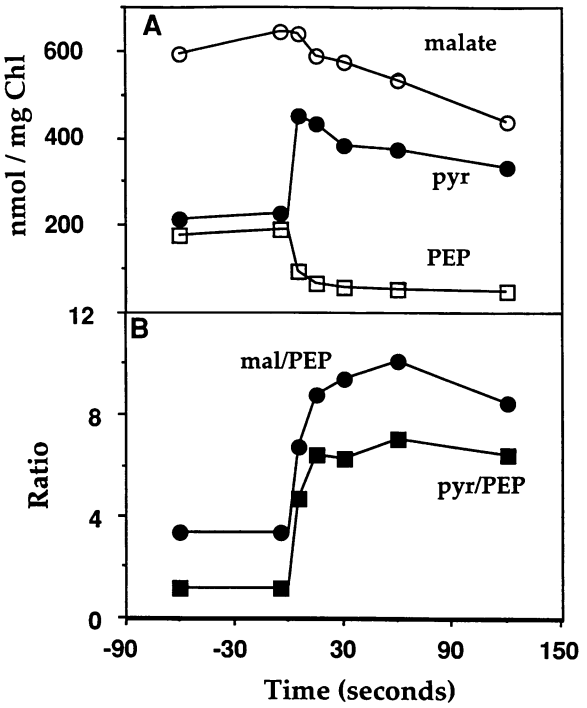

Figure 3. A, Changes in the cellular pool sizes of pyruvate, PEP, and malate in response to NH_4^+ addition at time 0. The data points represent the means of three separate experiments. B, Changes in the ratios of pyr/PEP and malate/PEP in response to NH_4^+ addition at time 0. The ratios are determined from the data in panel A.

Other Metabolites

Table I documents the changes in the pool sizes of the remaining metabolites assayed in the study. Following the addition of NH_4^+: RuBP levels fell by about 50%; triose-P levels rose by about threefold in parallel with FBP; citrate levels rose by about 1.5-fold; PGA levels fell by about 45% in parallel with PEP; and UDPGlc and isocitrate remained relatively constant.

DISCUSSION

N Assimilation by *N*-Limited *S. minutum*

When cells of *S. minutum* are cultured under N limitation their capacity for N assimilation increases dramatically. N-sufficient cells have maximal N assimilation rates of about 23 μmol N mg Chl^{-1} h^{-1} (4). In comparison, *N*-limited cells supplied with NH_4^+ are capable of sustained rates of NH_4^+ assimilation of up to 185 μmol N mg Chl^{-1} h^{-1} (27, 28) (see also "Results"). Primary N assimilation by green algae occurs via GS/GOGAT (3). GS catalyzes the ATP-dependent amidation of glutamate to glutamine. Figure 1 shows that the onset of NH_4^+ assimilation results in a rapid drop in glutamate and increase in glutamine, consistent with the operation of GS. The assimilation of N via GS/GOGAT requires ATP, reducing power and carbon skeletons in the form of αKG.

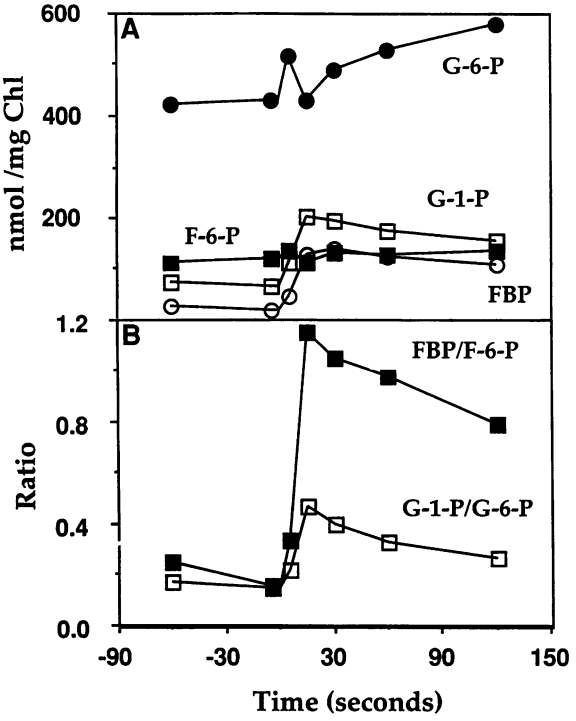

Figure 4. A, Changes in the cellular pool sizes of Glc-1-P, Glc-6-P, Fru-6-P, and FBP in response to NH_4^+ addition at time 0. The data points represent the means of three separate experiments. B, Changes in the ratios of Glc-1-P/Glc-6-P, and FBP/Fru-6-P in response to NH_4^+ addition at time 0. The ratios are calculated from the data presented in panel A.

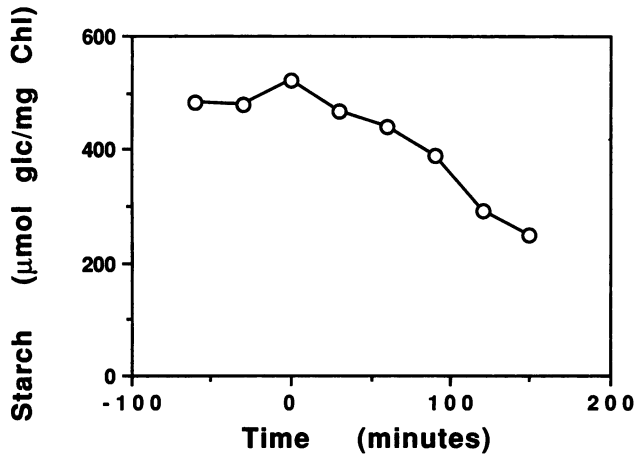

Figure 5. Changes in the cellular pool sizes of starch (in units of glucose equivalents) in response to NH_4^+ addition at time 0. The data points represent the means of three separate samples. Rates of starch and sucrose breakdown during N assimilation were 110 and 3.5 μmol Glc mg Chl^{-1} h^{-1}, respectively.

Consequently, alterations in cellular metabolism are expected so as to meet these new demands.

Response of Adenylates

Within 5 s of NH_4^+ addition, the effect of N assimilation on cellular ATP is apparent. ATP drops rapidly accompanied by reciprocal changes in ADP and AMP (Fig. 2). These results are similar to those reported by Ohmori and Hattori (17) for *Anabaena*. The changes in adenylates are transient, with recovery within 30 s nearly to the levels before N was added. As the rate of N assimilation remained high for considerable periods of time (Fig. 1) (27), this recovery suggests there must be an increase in the cells' capacity to generate ATP and/or a decrease in the rate of other ATP-consuming reactions. Weger *et al.* (27) have shown that NH_4^+ assimilation by *N*-limited *S. minutum* in the light results in a several fold increase in the rate of mitochondrial ETC activity. This enhancement in mitochondrial ETC activity was inhibited by cyanide, suggesting the engagement of cytochrome oxidase and a large increase in ATP production. At the same time, a decline in RuBP has been shown to cause a severe limitation in Calvin cycle activity (6), thus implying a decrease in a major ATP-consuming process. Although photosynthetic electron flow also declines, it does not decline to the same extent as photosynthetic carbon fixation (8), so the decrease in photosynthetic carbon fixation will also result in a relative increase in ATP availability. It is therefore likely that the rapid recovery in cellular ATP is due to (a) an increase in ATP production in the mitochondria and (b) a decreased ATP demand for photosynthetic carbon fixation.

The observation that the ATP/ADP ratio drops initially, while energization, as indicated by "high-energy state" quenching of Chl fluorescence, increases (8, 26), is somewhat unexpected. Two explanations might be offered for this divergence. On the one hand, it is possible that compartmentation of the adenine nucleotides means that the overall level does not reflect the ratio in the stroma. Alternatively, it is possible that the low ATP/ADP ratio and high energization are required to maintain the transiently high rate of ATP synthesis, via CF_1-ATP synthase, immediately after adding NH_4^+ and before the adjustments discussed in the previous paragraph come into operation. The high energization would be made possible by the proton-pumping associated with the rapid linear electron transport linked to the GOGAT reaction.

Table I. *Changes in Cellular Pool Sizes of Various Metabolites in Response to NH_4^+ Addition at Time 0*

The data represent the means of three separate experiments, the range about each value was generally in the range of 10 to 15%.

Metabolite	Time (s)						
	−60	−5	5	15	30	60	120
	nmol mg Chl^{-1}						
Alanine	165	146	154	146	178	219	276
PGA	1598	1591	1174	724	733	719	698
RuBP	344	280	135	102	126	119	100
Triose-P	57	58	70	119	146	142	203
Citrate	438	416	459	507	595	592	523
Isocitrate	11	8	8	7	8	10	8
UDPGlc	161	180	183	210	152	135	140

Provision of αKG for Net Glutamine/Glutamate Synthesis

The increase in net NH_4^+ assimilation via GS/GOGAT requires the provision of αKG. This is reflected by the rapid

decline of αKG within 5 s of NH_4^+ addition (Fig. 1). Within 15 s the rate of depletion of αKG declined, and by the end of the experiment, the pool stabilized at about 50% of control levels. The continued increase of glutamine, after glutamate and αKG had attained new quasiequilibrium levels, implied that the rate of αKG production had been increased. The rate of αKG production would have to be at least as great as the net rate of glutamine production. This suggests a major increase in *de novo* αKG production by the TCAC, which is consistent with the threefold increase in TCAC CO_2 release which accompanies NH_4^+ assimilation during photosynthesis by this organism (27, 28). It can also be noted that of all other detectable amino acids, only alanine showed any significant increase over the duration of the experiment. As this increase was minor relative to the increase in glutamine this implies that during the initial stages of NH_4^+-assimilation, regeneration of αKG through transamination of other organic acids is minor.

Increased TCAC activity and the use of TCAC intermediates in support of biosynthetic reactions will require an increase in both PK and PEPcase activity. Within 5 s of the addition of NH_4^+, there was a dramatic increase in pyr and a corresponding decrease in PEP. This resulted in a 7 fold increase in the pyr/PEP ratio (Fig. 3, A and B), a phenomenon previously implied from ^{14}C and ^{32}P labeling studies in a variety of plant systems (5, 10, 11, 19). As the change in pyr/PEP ratio occurs at the same time as a large increase in carbon flow through PK, this indicates that this enzyme is activated during NH_4^+ assimilation. The cytosolic isozyme of PK from *S. minutum* has been purified to near homogeneity (13) and found to be inhibited by glutamate and activated by dihydroxyacetone phosphate (14). During NH_4^+ assimilation the rapid drop in glutamate and increase in triose-P (Fig. 1; Table I), most of which is dihydroxyacetone phosphate, suggests that this mechanism of PK regulation may provide the immediate explanation for the increase in carbon flow through this enzyme. The increase in carbon supply to the TCAC via PK is consistent with the decline in malate and an increase in citrate (Fig. 3A; Table I).

Sustained anabolic TCAC activity will also require an increase in PEPcase activity. The *in vivo* rate of PEPcase activity is difficult to determine during photosynthesis due to the simultaneous fixation of carbon by ribulose-1,5-bisphosphate carboxylase/oxygenase. However, recent studies, using $^{13}C/^{12}C$ discrimination (7) and radiolabel localization techniques (5), have shown that the activity of PEPcase increases dramatically during NH_4^+ assimilation in the light. These findings coupled with the change in malate/PEP ratio reported here (Fig. 3B), implies that PEPcase is also activated rapidly during NH_4^+ assimilation, although the mechanism of its regulation is not yet known.

Increased Mitochondrial ETC Activity during N Assimilation

The increase in TCAC carbon flow is supported by an increase in mitochondrial ETC activity (27). It is thought that increased mitochondrial ETC activity can occur as a response to either increases in ADP or substrate supply (12). Although there is a transient increase in ADP immediately following NH_4^+-addition (Fig. 2), it returns to near control values within 120 s. As ETC activity remains high long after ADP has declined, these results suggest that although ADP may play a role in the initial enhancement of mitochondrial ETC activity, the sustained increase may, rather, be due to the increased provision of NADH from the TCAC.

Source of Carbon for NH_4^+ Assimilation: Regulation of Starch Metabolism and Glycolysis

The sustained assimilation of NH_4^+ at rates of up to 185 μmol mg^{-1}Chl h^{-1} (28) requires the mobilization of large quantities of organic carbon. This demand could be met, in part, by the redirection of recent photosynthate from starch synthesis to organic acid and amino acid production (10). However, even a complete redirection of photosynthate would not be able to cope with the very high rates of N assimilation found in our experiments. Indeed, during NH_4^+ assimilation by *N*-limited *S. minutum* the Calvin cycle is actually severely inhibited (Table I) (6), thus decreasing the availability of new photosynthate. As a result the major sources of organic carbon for amino acid synthesis comes from mobilized starch and sucrose. NH_4^+ assimilation causes degradation of starch and sucrose (Fig. 5) (10, 15). The rate of starch degradation reported here (110 μmol Glc mg Chl^{-1} h^{-1}) was over 30-fold greater than that of sucrose degradation. This indicates that starch degradation supplies most of the carbon skeletons required during N assimilation.

Glc-1-P is an initial product of starch degradation and has been thought to be in equilibrium with chloroplastic Glc-6-P. Recently, it has been shown (22) that the chloroplastic phosphoglucomutase may not be able to maintain this equilibrium during periods of rapid starch degradation, suggesting that the observed increase in the Glc-1-P/Glc-6-P ratio may reflect the onset of rapid starch breakdown. Such an increase in Glc-1-P relative to Glc-6-P was observed within 5 s of NH_4^+ addition (Fig. 4, A and B) suggesting that the initiation of starch breakdown is extremely rapid. This increase in Glc-1-P/Glc-6-P was verified by both the Glc-6-P-dehydrogenase and UDPGlc-dehydrogenase assays. Presumably, the rapid mobilization of starch could result from an inhibition of starch synthesis as well as an increase in the rate of starch degradation (24). ADPGlc pyrophosphorylase catalyzes the rate-limiting reaction in the pathway to starch synthesis. In *Chlorella*, and other plant systems, this enzyme is less active when ATP/ADP and PGA/Pi ratios are low (16, 24). In *S. minutum*, the ATP/ADP ratio (Fig. 2) and the PGA level (Table I) both decreased during NH_4^+ assimilation, implying that ADPGlc pyrophosphorylase may be inactivated and the rate of starch synthesis decreased. Unfortunately, the regulatory mechanisms involved with the degradation of starch have not yet been identified (23).

The carbon flow through glycolysis must also increase during NH_4^+ assimilation. The increase of FBP and triose-P, relative to Fru-6-P (Fig. 4, Table I) is certainly consistent with an activation of glycolysis. However, it is not yet known at what stage the products of starch mobilization are leaving the chloroplast, thus it is not possible to elucidate whether this involves activation of the chloroplast PFK, or the cytosolic PFK, or even phosphofructophosphotransferase (EC

2.7.1.90). In this context, we have observed that αKG is an effective inhibitor of PFK in crude extracts of *S. minutum* in the mM concentration range (Stitt and Turpin, unpublished data), suggesting that the decline of αKG after adding NH_4^+ (Fig. 1) could contribute to the activation of glycolysis. It should also be noted that an activation of glycolysis would also require that the corresponding FBPases are inactivated (see also below).

Regulation of the Calvin Cycle

During transient NH_4^+ assimilation by *N*-limited *S. minutum*, photosynthetic carbon fixation becomes limited by the RuBP concentration (6). Since the rate of carbon export from the chloroplast is greater than that which can be sustained by the fixation of new carbon (5), it was hypothesized that the decrease in RuBP may result from the depletion of Calvin cycle intermediates due to their export in support of NH_4^+ assimilation. If this hypothesis is correct, we should observe a decrease in the metabolites downstream of triose-P, specifically FBP. What is observed, however, is a large increase in cellular FBP. This provides evidence that a "triose-P drain" is not responsible for the inhibition of the Calvin cycle.

Rather, the increase in cellular triose-P and FBP indicate that the decrease in Calvin cycle activity may be due to the direct regulation of one or more of its enzymes. The increase in FBP and decline in RuBP suggests that the regulatory step must be downstream of FBPase and at or upstream of phosphoribulokinase. Three regulatory enzymes may serve this function: FBPase, sedoheptulose-1,7-bisphosphatase (EC 3.1.3.37), and phosphoribulokinase. It is unlikely that inhibition of FBPase alone could account for the observed changes in photosynthetic carbon fixation as there is rapid starch degradation after adding NH_4^+ (Fig. 5). This would effectively bypass the FBPase step by providing Fru-6-P. Hence, SBPase and phosphoribulokinase are more likely candidates for serving this regulatory function. Analyses of further metabolites over even shorter time periods to identify this site of regulation are currently underway.

ACKNOWLEDGMENTS

We would like to thank Ulrich Schurr for carrying out the amino acid analysis and Dieter Sultemeyer for transporting some samples from Canada to FRG.

LITERATURE CITED

1. **Bassham JA, Larsen PO, Lawyer AL, Cornwell KL** (1981) Relationship between nitrogen metabolism and photosynthesis. *In* JD Bewley, ed, Nitrogen and Carbon Metabolism. Dr W. Junk, London, pp 135–163
2. **Bergmeyer U** (1972) Methoden der enzymatischen Analyse, Vol 2. Verlag Chemie, Weinheim, Bergctr, pp 1624–1627
3. **Cullimore JV, Sims AP** (1982) Glutamine synthetase of *Chlamydomonas*: its role in the control of nitrate assimilation. Planta **153:** 18–24
4. **Elrifi IR, Turpin DH** (1986) Nitrate and ammonium induced photosynthetic suppression in *N*-limited *Selenastrum minutum*. Plant Physiol **81,** 273–279
5. **Elrifi IR, Turpin DH** (1987) The path of carbon flow during NO_3^--induced photosynthetic suppression in *N*-limited *Selenastrum minutum*. Plant Physiol **83:** 97–104
6. **Elrifi IR, Holmes JJ, Weger HG, Mayo WP, Turpin DH** (1988) RuBP limitation of photosynthetic carbon fixation during NH_3 assimilation: interactions between photosynthesis, respiration and ammonium assimilation in *N*-limited green algae. Plant Physiol **87:** 395–401
7. **Guy RD, Vanlerberghe GC, Turpin DH** (1989) Significance of phosphoenolpyruvate carboxylase during ammonium assimilation: carbon isotope discrimination in photosynthesis and respiration by the *N*-limited green alga *Selenastrum minutum*. Plant Physiol **89:** 1150–1157
8. **Holmes JJ, Weger HG, Turpin DH** (1989) Chlorophyll *a* fluorescence provides an accurate measure of total photosynthetic electron flow to CO_2 or NO_3^-/NO_2^- under transient conditions. Plant Physiol (in press)
9. **Jones MGK** (1981) Enzymatic assay for starch and glycogen. *In* H Kornberg J Metcalfe, D Northcote, C Pogson, K Tipton, eds, Techniques in Carbohydrate Metabolism. Elsevier/North-Holland, Amsterdam, pp. 1–13
10. **Kanazawa TK, Kanazawa K, Kirk MR, Bassham JA** (1970) Regulatory effects of ammonia on carbon metabolism in photosynthesizing *Chlorella pyrenoidosa*. Biochim Biophys Acta **205:** 401–408
11. **Kanazawa TK, Kanazawa K, Kirk MR, Bassham JA** (1972) Regulatory effects of ammonia on carbon metabolism in *Chlorella pyrenoidosa* during photosynthesis and respiration. Biochim Biophys Acta **265:** 656–669
12. **Lambers H** (1989) The oxidation of mitochondrial NADH and production of ATP. *In* DT Dennis, DH Turpin, eds, Advanced Plant Biochemistry and Molecular Biology. Longman Press (in press)
13. **Lin M, Turpin DH, Plaxton WC** (1989) Pyruvate kinase isozymes from the green alga, *Selenastrum minutum*. I. Purification and physical and immunological characterization. Arch Biochem Biophys **269:** 219–227
14. **Lin M, Turpin DH, Plaxton WC** (1989) Pyruvate kinase isozymes from the green alga, *Selenastrum minutum*. II. Kinetic and regulatory properties. Arch Biochem Biophys **269:** 228–238
15. **Miyachi S, Miyachi S** (1985) Ammonia induces starch degradation in *Chlorella* cells. Plant Cell Physiol **26:** 245–252
16. **Nakamura Y, Imamura M** (1985) Regulation of ADP-glucose pyrophosphorylase from *Chlorella vulgaris*. Plant Physiol **78:** 601–605
17. **Ohmori M, Hattori A** (1978) Transient change in the ATP pool of *Anabaena cylindrica* associated with ammonia assimilation. Arch Microbiol **117:** 17–20
18. **Ohmori M, Miyachi S, Okabe K, Miyachi S** (1984) Effects of ammonia on respiration, adenylate levels, amino acid synthesis and CO_2 fixation in cells of *Chlorella vulgaris* 11 h in darkness. Plant Cell Physiol **25:** 749–756
19. **Platt SG, Plaut Z, Bassham JA** (1977) Ammonia regulation of carbon metabolism in photosynthesizing leaf discs. Plant Physiol **60:** 739–742
20. **Quick WP, Neuhaus E, Feil R, Stitt M** (1989) Fluoride leads to an increase of inorganic pyrophosphate and an inhibition of photosynthetic sucrose synthesis in spinach leaves. Biochim Biophys Acta **973:** 263–271
21. **Schurr U, Gebauer G** (1989) Amino acid measurement with OPA derivatization on precolumns. *In* Aplikacion Communikation Information Hanszeitschrift Derkontron Instruments 3 (in press)
22. **Sicher R** (1989) Evidence for a light dependent increase of phosphoglucomutase activity in isolated, intact spinach chloroplasts. Plant Physiol **89:** 557–563
23. **Steup M** (1988) Starch degradation. *In* PK Stumpf, EE Conn, eds, The Biochemistry of Plants: A Comprehensive Treatise, vol 14, Academic Press, New York, pp 255–296
24. **Stitt M, Heldt HW** (1981) Simultaneous synthesis and degradation of starch in spinach chloroplasts in the light. Biochim Biophys Acta **638:** 1–11
25. **Turpin DH, Elrifi IR, Birch DG, Weger HG, Holmes JJ** (1988) Interactions between photosynthesis, respiration, and nitrogen assimilation in microalgae. Can J Bot **66:** 2083–2097

26. **Turpin DH, Weger HG** (1988) Steady-state chlorophyll*a* fluorescence transients during ammonium assimilation by the N-limited green alga *Selenastrum minutum*. Plant Physiol **88:** 97–101
27. **Weger HG, Birch DG, Elrifi IR, Turpin DH** (1988) Ammonium assimilation requires mitochondrial respiration in the light. A study with the green alga *Selenastrum minutum*. Plant Physiol **86:** 688–692
28. **Weger HG, Turpin DH** (1989) Mitochondrial respiration can support NO_3^- and NO_2^- reduction during photosynthesis: interactions between photosynthesis, respiration and N assimilation in the *N*-limited green alga *Selenastrum minutum*. Plant Physiol **89:** 409–415
29. **Wintermans JFGM, De Mots A** (1965) Spectrophotometric characteristics of chlorophylls *a* and *b* and their phaeophytins in ethanol. Biochim Biophys Acta **109:** 448–453.
30. **Wirtz W, Stitt M, Heldt HW** (1980) Enzymatic determination of metabolites in the subcellular compartments of spinach protoplasts. Plant Physiol **66:** 187–193